Available online at www.sciencedirect.com
ScienceDirect
Applied Catalysis B: Environmental 78 (2008) 250–258
APPLIED CATALYSIS B: ENVIRONMENTAL
www.elsevier.com/locate/apcatb

Photo-Fenton degradation of 17β-estradiol in presence of α-FeOOHR and H_2O_2

Zhao Yaping [a,b], Hu Jiangyong [a,*]

[a] Division of Environmental Science and Engineering, National University of Singapore, 119260 Singapore, Singapore
[b] Department of Environmental Science and Technology, East China Normal University, Shanghai 200062, China

Received 27 April 2007; received in revised form 12 September 2007; accepted 14 September 2007
Available online 29 September 2007

Abstract

A novel photocatalyst, α-FeOOH-coated resin (α-FeOOHR), was prepared and applied for the photodegradation of natural estrogen 17β-estradiol (E2) in presence of H_2O_2 under the relatively weak UV irradiation. The continuing loading of ferric oxide on resin was achieved by in situ hydrolysis of Fe^{3+} in alkaline solution. The effects of initial pH, catalyst loading, oxidant concentration and iron leaching on the photodegradation of E2 were investigated. The batch photodegradation experiment showed that high removal efficiency of E2 and fairly good mechanic stability could be obtained by the spherical photocatalyst α-FeOOHR in aqueous solutions. The photodegradation efficiencies slightly decreased with the increase of initial pH in the wide pH range of 3–11. Increase of oxidant and catalyst will enhance photodegradation efficiencies thus lead to increase the Ferric leaching. Neglected iron leaching showed the stability of the loaded α-FeOOH withstanding the oxidation. X-ray photoelectron spectrum (XPS) shed light on the surface activity change of photocatalyst and heterogeneous catalytic essence of this process.

Keywords: 17β-Estradiol; α-FeOOH-coated resin; Heterogeneous; Fenton reaction; Photocatalysis

1. Introduction

Endocrine disruptor compounds (EDCs) have become one of the 'hottest' topics in environmental science today, especially within these few years. They may interfere with the normal functioning of endocrine systems, thus affecting the reproduction and development in wildlife and humans [1–3]. Among the EDCs, natural estrogens are thought to be most likely to cause estrogenic effect on aquatic life at environmentally relevant concentration. 17β-Estradiol (E2), mainly concerned natural estrogen due to its potent estrogenicity, is ubiquitous in the aquatic environment systems. The concentration of E2 detected in surface water was usually near or below 2 ng/L, while in effluent wastewater E2 concentration ranged from below detection limit to 64 ng/L [4]. E2 has been reported experimentally to exhibit some estrogenic activity for human estrogen receptors at 41 ng/L [5] and even to cause vitellogenin production in male fish at environmental concentration of 1.0 ng/L [6]. However, current wastewater treatment methods, such as activated sludge process, are ineffective in removing these substances from wastewater [7–9]. Therefore, it has become an emergent issue to focus on developing effective method for removing E2 in aquatic environment to the level that does not pose public health risk.

Various forms of advance oxidation processes (AOPs) have emerged as important alternatives for efficient mineralization of these EDCs [10–13]. Fenton process has its own unique advantages as an oxidizing process because its reagents are inexpensive, environmentally benign and relatively easy to transport and handle. The homogeneous Fenton process is efficient only in the pH range of 2–4 and is usually most efficient at around 2.5–3 but rather inefficient in the pH range of most natural waters (pH 5–9). This is particularly due to the tendency for ferric oxyhydroxide precipitation, which has a low catalytic activity, to occur at pH > 3–4 depending on the iron concentration [14,15]. While for heterogeneous Fenton process, the source of iron used as a catalyst can be a solid surface, including iron-containing minerals or iron-coated particles. The heterogeneous system has more advantages than the homogeneous Fenton reagent from the viewpoints of the

* Corresponding author. Tel.: +65 6516 4540; fax: +65 6774 4202.
E-mail address: esehujy@nus.edu.sg (H. Jiangyong).

0926-3373/$ – see front matter © 2007 Elsevier B.V. All rights reserved.
doi:10.1016/j.apcatb.2007.09.026

reaction pH range and the removal of iron ions. For heterogeneous processes, many reactions thus occur at the solid–liquid interface. In this case, significant reduction in dissolved Fe can be achieved by the use of heterogeneous Fenton processes, where the iron remains substantially in the solid phase, either as a mineral or as an adsorbed ion. The catalyst enables operation at around neutral pH with close to equal efficiency as that in acidic solutions.

In recent years, iron(III) (hydr)oxides (hematite, α-Fe_2O_3 and goethite and α-FeOOH) as heterogeneous catalysts attracted great interests among researchers [16,17]. Goethite is naturally occurring mineral and is widely available. Goethite is almost insoluble in aqueous media over a wide pH range. So it can be able to function as a heterogeneous catalyst without losing a substantial amount of its mass. He et al. reported the photodegradation of an azo using goethite and thought production of surface Fe(IV) species and hydroxyl radicals ($^{\bullet}$OH) when UV irradiation of the surface broke the FeO–OH bond. Then the highly oxidized and unstable oxoiron (Fe(IV)) reacted with water to form a further $^{\bullet}$OH [18,19]. Then the dyes adsorbed on the surface of the goethite were oxided by $^{\bullet}$OH. But this kind of photocatalytic reaction is usually carried out in the slurry system under UV irradiation, as they usually appear as fine powders, which cannot be applied in fixed-bed columns unless they are of a granular shape. The slurry system compared with immobilize system has many drawbacks, the small particle size catalysts have to be removed afterwards, usually by filtration or centrifugation which is a long and costly procedure and would be a factor to consider on an industry scale.

Supported iron compounds are another type promising catalysts, the supporters can be organic and inorganic materials, such as ZSM-5 zeolite [20], activated carbon [21], alginate gel beads [22], Nafion membrane [23], cationic exchange resin [24,25], etc. Fajerwerg et al. [20] presented Fe–ZSM-5 (2.0 wt.% Fe and particle size 1 μm) could eliminate total phenol in presence of H_2O_2 under mild working conditions. Moreover, it remained active after successive runs. But the leached iron was up to 6 mg/L after 3 h reaction at pH 5, which directly reflected the instability of catalyst. They also compared photoactivity of Fe–ZSM-5 zeolite with the silica/Fe-structured silica and found phenol conversion activity of silica/Fe-structured silica was less than that of Fe–ZSM-5, while iron ions leached was higher. Vaughan et al. [23] reported the degradation of 2,4-dichlorophenol by Fe-immobilized Nafion membrane (1.78 wt.% Fe) in presence of H_2O_2 under solar simulated visible light irradiation. The Nafion membrane seemed effective over many cycles photodegradation at wide pH range (between 2.8 and 11) without leaching out of a significant amount iron ion. But the price of Nafion membrane is expensive. It also cannot stand the oxidation by $^{\bullet}$OH. Usually, the photocatalytic activity is closely linked with the content of iron ions on the supporters. The maximum mass percent of iron loaded reached only 0.1–5% for sands, activated carbon, zeolite [26] and Nafion membrane and at the same time they had some extent iron leached phenomenon. Iron content is one of the most important indexes to evaluate the photo-activity of catalysts. The shortcoming of these catalysts will significantly affect the catalytic activity, stability and lifetime. Exchange resin with special functional groups, such as sulfonic, was also chosen as supporters because it can immobilize large amount of iron up to 9–12 wt.% Fe within polymer matrix [24,25]. Besides this, the iron-immobilized resins have other superiorities: the first is iron compounds agglomerates are irreversibly encapsulated within the spherical exchanger. Turbulence and mechanical stirring do not result in the loss of Fe compounds particles whatsoever [24]; the second is polymeric cation exchanger is one of the most inexpensive, durable and widely available adsorbents throughout the world. Use of this material as the primary substrate is likely to make adsorbent cost competitive with other adsorbent already available commercially.

Recently, some authors reported that the Fe(III)-exchanged resin was an effective catalyst for the degradation of dyes under visible light irradiation in the presence of H_2O_2 [27,28]. Although Fe(III)-immobilized chelating resin has high photo-efficiency, it still faces a serious problem of notable dissolution of Fe(III) into the solution upon UV irradiation and H_2O_2 oxidation. Lv et al. [27] reported the leakage rate of Fe(III)-exchanged resin surpassed 5.5% when the concentration of supported Fe(III) was 16.2 mg/L. At the same time, the photodegradation efficiency decreased greatly with increase of pH in this report. In order to decrease the iron leakage and improve photocatalyst's stability and catalytic efficiency within a wide pH range, we explored a novel heterogeneous Fenton photocatalyst of α-FeOOH-coated resin (α-FeOOHR) and evaluated the catalytic activity for the degradation of E2 in the presence of H_2O_2 under relatively weak irradiation in aqueous solution.

2. Experimental

2.1. Chemicals

17β-Estradiol (>98%; Sigma, 272.4 g/mol) was used without further purification. All the other chemicals used were analytical grade and all the solvents used were HPLC grade. The water employed was purified by a Milli-Q system with a resistivity higher than 18.2 MΩ cm at 25 °C. The resin was Amberlite® 200 with matrix of styrene-divinylbenzene, Na^+-form, strongly acidic and particle size of 20–50 mesh (0.297–0.840 mm) (Fluka). Goethite was with a specific surface 215 m^2/g and particle size of 200–325 mesh (0.074–0.044 mm) with ∼35% iron content (Fluka). 0.1 mM stock solution was prepared by dissolving desired amount of E2 into methanol and stored in 4 °C. Working solutions were followed by diluting stock solution with Milli-Q water to desired concentrations.

2.2. Preparation and characterization of α-FeOOHR catalyst

The catalyst was prepared by dissolving 2 g $FeCl_3 \cdot 6H_2O$, 5 g carbamide and 10 mL resin into 100 mL doubly distilled water, then refluxed and were allowed to grow on the surfaces of resin for 7 days. After repeated washing with doubly distilled water and alcohol, the formed α-FeOOHR was desiccated under

ambient temperature and stored in polyethylene bottles for further use. The physiochemical parameters were characterized by X-ray diffraction (XRD-6000) and scanning electron microscopy (SEM). Phase composition and crystallization of the α-FeOOHR were examined by XRD using a Philips PW 1729 type X-ray diffractometer with Cu Kα radiation (Shimadzu, Japan). Surface morphology was observed by SEM, using a JEOL 6700F type field emission scanning electron microscope with magnification up to 650,000× and the resolution of 1 nm (JEOL, Japan). The iron content was determined by Shimadzu AAS-6700 (Shimadzu, Japan). X-ray photoelectron spectrum (XPS) was performed in a Kratos AXIS Hsi, Mono Al Kα system, energy is 1486.71 eV (Kratos Analytical, Japan).

2.3. Photo-Fenton experiments

The photochemical reactor was made of open cylindrical Pyrex with diameter 19 cm and height 9 cm and equipped with a magnetic stirring bar. One litre of E2 aqueous solution with desired concentration was added without adjusting pH prior to the addition of required amount of α-FeOOHR (5 g/L and 0.5 g Fe/L) and H_2O_2 (9.7 mM). The mixture was magnetically stirred at 200 rpm at 20 °C air-cooled room. The irradiation was carried out with two 15 W black light lamps (Wuxing Co., Singapore) with the irradiation intensity at the center of the reactor of 0.3 mW/cm^2 (measured by use of a UV radiometer, IL700, International Light, USA) and the main emission wavelength of 365 nm. The distance between light source and the surface of the solute was 5 cm. About 15 mL aliquot of the suspension was collected at regular intervals and analyzed for subsequent residual E2 concentrations, pH and total dissolved iron. In addition to photocatalysis, blank photolysis experiment, control experiments and the effects of pH, H_2O_2 concentration and α-FeOOHR loading on E2 degradation were carried out under the same conditions as indicated above.

2.4. Analyses

All the photodegradation samples were concentrated by solid-phase extraction (SPE) with C18-M cartridge (Strata™ C18-M, 10 mm × 5 mm inside diameter disposable precolumns that contained 30 mg of sorbent, Phenomenex, USA) on the cartridge exchange module. The cartridges were conditioned sequentially with 5 mL of methanol and 10 mL of Milli-Q water. Afterwards, a 10 mL aliquot of water sample was preconcentrated through the cartridge. Finally, the compounds trapped on the adsorbent were eluted into the bottles with dichloromethane after washing with 5 mL Milli-Q water and 5 mL hexane. The eluant was followed by N_2 gas bubbling and dissolved in methanol.

The amount of E2 in the test solutions was determined with a liquid chromatography/triple quadrupole tandem mass spectrometry, equipped with turbo ion spray interface (API2000 LC/MS/MS system, Applied Biosystems Asia Pvt. Ltd., USA). HPLC series 1100 (Agilent) is equipped with a reversed-phase C18 analytical column (Zorbax SB-C18, USA) of 150 mm × 2.1 mm and 3.5 μm particle diameter. Column temperature was maintained at 22 °C. The mobile phase used for eluting E2 from the HPLC columns consisted of acetonitrile and water (30:70, v/v) at a flow rate of 0.3 mL/min. The MS/MS turbo ion spray interface was operated in the negative ion mode at 4500 V and 450 °C. Nitrogen as the nebulizing and drying gas was generated from compressed air using a Kaken N_2 generator (System Instruments Co. Ltd., Japan). The ion sources gas 1 (GS1) and 2 (GS2) were set at 40 L/min and 90 L/min, respectively. The curtain gas (CUR) flow was set at 30 L/min and the collision gas (CAD) at 6.0 L/min. Quantification was performed by multiple reaction monitoring (MRM) of the deprotonated precursor molecular ions $[M–H]^-$ and the related product ion for E2. Quadrupoles Q1 and Q3 were set on unit resolution. MRM in the negative ion mode was performed using a dwell time of 100 ms per transition to detect ion pairs. Table 1 shows the optimized MS/MS conditions for E2. LC/MS/MS data were processed by Analyst Software 1.4.1 (Applied Biosystems, Applied Biosystems Asia Pvt. Ltd., USA). Quantitation of the samples was carried out under MRM conditions by using the corresponding peak areas. Standard working curve based on mean HPLC peak areas counts was constructed.

Table 1
Optimum conditions for MS/MS (ESI negative ion mode) analysis of E2

MW	272
m/z	
Q1 mass	271.0
Q3 mass	145.1
DP (V)	100
EP (V)	12
CE (V)	60
CXP (V)	5

3. Results and discussion

3.1. Characterization of catalyst

Amberlite® 200, spherical macroporous cationic exchange resin of polystyrene matrix with sulfonic acid groups, was chosen as photocatalyst carriers. The crystalline of the loaded iron oxide on the resin was characterized by XRD in high angle range depicted in Fig. 1. Comparing with the standard PDF database, the XRD spectrum showed that the iron oxide crystalline is the typical pattern of crystalline α-FeOOH (goethite, syn). No characteristic peak was observed for other impurities, such as hemitate and β-FeOOH. The morphology of resin beads, surface of resin and surface of α-FeOOH entities was analyzed by SEM shown in Fig. 2. SEM also confirmed the presence of α-FeOOH entities on the surface of resin comparing with non-coated resin (one note is that the gap on the surface of resin caused by the high vacuum of SEM machine). The α-FeOOH entities were mainly one-dimensional nanobars with cross section of 100 nm × 100 nm and length 300–400 nm except for few irregular micrometer particles.

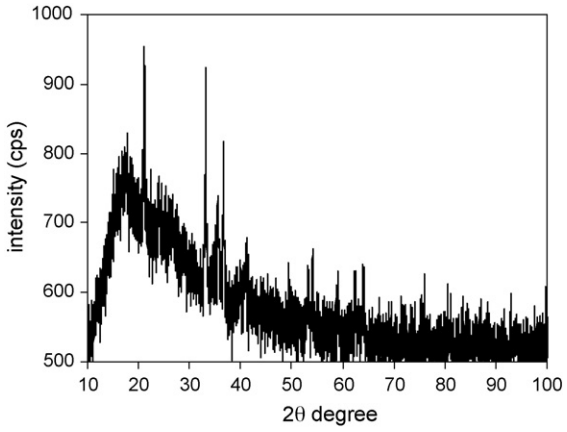

Fig. 1. XRD pattern of the α-FeOOHR.

The α-FeOOH particles loaded was found inside the pores of polymer matrix by in situ hydrolysis of Fe(III) ions. The loaded α-FeOOH in the photocatalyst was digested by HNO_3–HCl and the iron content measured by AAS was 10 wt.% Fe, i.e.100 mg Fe/g photocatalyst. The loaded α-FeOOH content in polymer matrix could be comparable to DeMarco's work, who reported iron loaded on macroporous polystyrene beads functionalized with sulfonic acid groups could be 9–12 wt.% Fe [25]. Ion exchange resin supporters showed higher chelating ability than that of inorganic carriers, such as zeolite, sand and silica whose iron loaded contents were less than 5 wt.% Fe and also not stable [26]. Iron content is one of the most important factors to influence the photoactivity of catalysts. High iron content of Fenton catalyst will inevitably increase the photocatalytic efficiency.

3.2. Photo-Fenton catalysis experiments and photolysis experiments

The efficiency of α-FeOOHR catalyst with or without photo-assisted degradation of E2 was evaluated under different experimental conditions. Fig. 3 shows the E2 decomposition with time under different conditions. The photocatalytic ability of α-FeOOHR in presence of H_2O_2 (curve 5) showed a significant E2 reduction achieving a residual E2 concentration of 36.9 μg/L, or a conversion rate of 86.4% after 8 h reaction. In absence of H_2O_2 in analogous reaction condition (curve 2) it led to residual E2 concentration of 125.8 μg/L, or a conversion rate of 53.8%. E2 reduction was also observed in dark Fenton reaction only in presence of α-FeOOHR and H_2O_2 (curve 3), the residual E2 concentration was 162.9 μg/L with a conversion rate of 40.1%. The small extent degradation in dark Fenton reaction may be due to the formation of hydroxyl radical by thermal decomposition of H_2O_2 [29]. So the dark Fenton reaction showed that the production of hydroxyl radicals were restricted without UV irradiations. The photolysis in presence of H_2O_2 (curve 1) yielded an enhanced rate of E2 decomposition with residual E2 concentration of 200.0 μg/L and a conversion rate of 26.5%, which showed that H_2O_2 also could go upon photolysis yielding hydroxyl radicals under 365 nm light irradiation [30]. The results suggested that UV irradiation would further accelerate the photodegradation rate. He et al. [19] also proved that the UV irradiation could accelerate the degradation of organic dye in aqueous H_2O_2/α-FeOOH dispersions owing to the enhancement of hydroxyl radicals comparing to that in the dark. Finally, the photocatalytic ability of α-FeOOHR was compared with commercial goethite (curve 4), with the same content of Fe(III) ions under the same condition. A lower E2 conversion rate of 38.7% with a residual E2 concentration of 166.8 μg/L was obtained by goethite catalyst. This may be ascribed to the presence of a significant

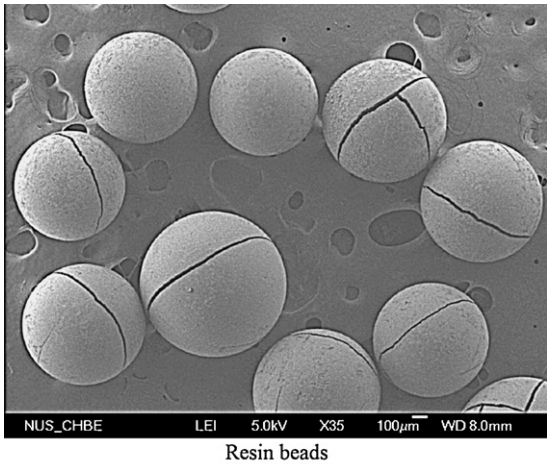

Resin beads

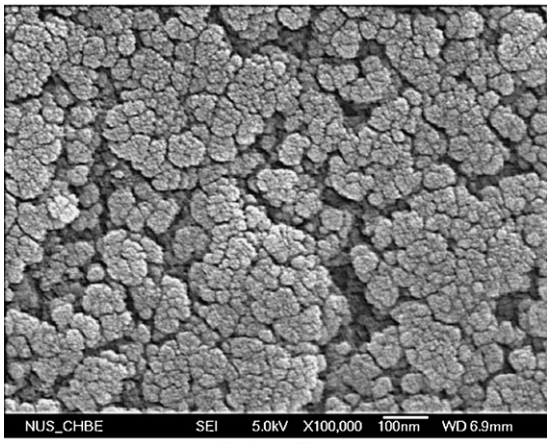

Resin surface

α-FeOOHR surface

Fig. 2. SEM surface image.

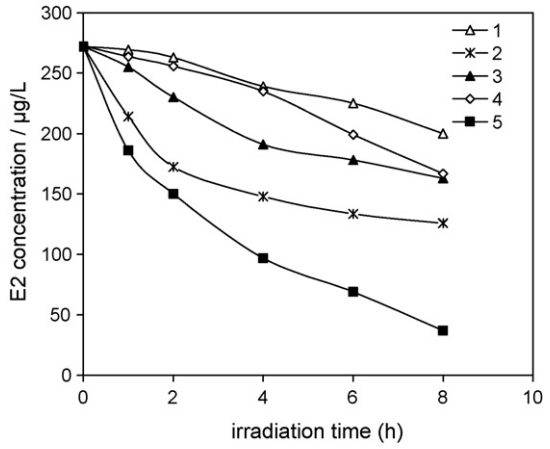

Fig. 3. Degradation of E2 along time under different conditions. $[E2]_0$ = 272 μg/L; $[H_2O_2]$ = 9.7 mmol/L; [goethite] = 1.43 g/L (0.5 g Fe^{3+}/L); [α-FeOOHR] = 5 g/L (0.5 g Fe^{3+}/L); pH 7.47; T = 20°C. Photodecomposition of E2 under different conditions: (1) photolysis in presence of H_2O_2; (2) photocatalysis in presence of α-FeOOHR; (3) dark-Fenton reaction in presence of α-FeOOHR and H_2O_2; (4) photocatalysis in presence of goethite and H_2O_2; (5) photocatalysis in presence of α-FeOOHR and H_2O_2.

amount of solid particle, which would reduce the transmission of near UV–vis light and produce scattering of the incident light reaching surface of goethite thus decreased photoactivity [31,32]. The better photodegradation efficiency of α-FeOOHR showed that α-FeOOHR would be an efficient photocatalyst.

3.3. Factorial effects of photo-Fenton catalysis experiments

3.3.1. Effect of pH

The effects of pH on the percentage of E2 with α-FeOOHR were determined with a pH range of 3–11 and results were presented in Fig. 4. In this study, the photodegradation process remained efficient and feasible up to pH 11.00 with the photodegradation rate of E2 remaining 63.2% comparing with 98.2% at pH 3.07 and 86.4% at pH 7.47. This suggests that heterogeneous Fenton catalyst can overcome the drawback of a narrow pH range of conventional Fenton reaction. From the point of pH_{zpc} it can be explained that photodegradation

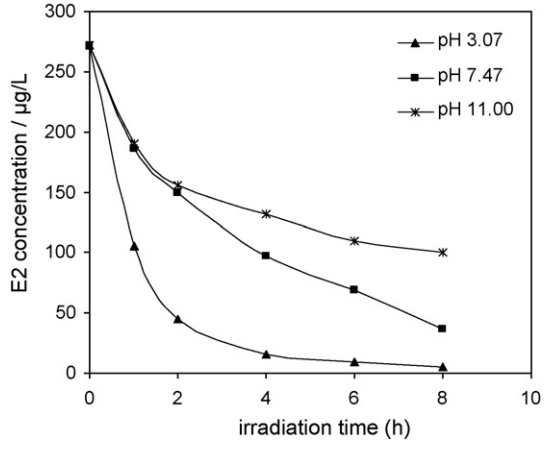

Fig. 4. The effect of pH on photodegradation of E2. $[H_2O_2]$ = 9.7 mmol/L; [α-FeOOHR] = 5 g/L; T = 20°C; pH 3.07, 7.47 and 11.00.

efficiency of E2 decreased with increase of pH. Iron oxides, whether they can be identified as having a particular crystal structure or not, typically have PZCs in the pH range of 7–9 [33–36]. α-FeOOH is positively charged at $pH < pH_{zpc}$ and favors E2 adsorption [19]. E2 would be ionized to the phenoxide and also the surface of α-FeOOH is deprotonated to the negative ions causing repulsion with substrate when $pH > pH_{zpc}$, especially pH > 10 (pK_a of E2) [37]. The variation of photodegradation rate with pH may also be explained in part by different surface species of FeOOH due to the dissociation of FeOOH in water, i.e. ≡Fe–OH_2^+, ≡Fe–OH and ≡Fe–O^- (the dissociation constant of FeOOH is K_{a1} = 5.3 and K_{a2} = 8.8, respectively). Different species maintains a different level of binding strength with H_2O_2 and E2, and the binding strength may be altered with pH [38]. Many studies had reported that solution pH dramatically influence homogeneous Fenton reaction efficiency. The results showed that the reaction efficiency of homogeneous Fenton process tended to be highest at around pH 3 and decreased with increasing pH. At neutral pH the homogeneous photodegradation efficiency can nearly be neglected because of the iron precipitation, for example, negligible degradation removal efficiency of <5% took place at pH > 8 when BPA was degraded by modified homogeneous Fenton process [33]. Neppolian reported that the *p*-CBA degradation by FeOOH/H_2O_2 indicated the 38% degradation at pH 3, 9% and 4% at pH 7 and 9 [34].

Generally, the pH change can have an obvious effect not only on the mode of adsorption of substrate on the catalyst but also on the selectivity of the photodegradative reaction on the catalyst surface. So the heterogeneous Fenton reactions can also be extensively influenced by pH. Lv et al. [27] had reported dyes degraded by photo-assisted Ferric loaded resin. The reaction performed at pH from 2 to 10 of the degradation rate decreased so quickly with increase of initial pH, for example, the removal efficiency of MG from 75.4% decreased to 3.41% when pH increased from 2.0 to 10.0. He et al. [19] reported the effect of pH on the photodegradation of salicylic acid in H_2O_2/goethite system. The detrimental effect of pH was also obvious. The efficiency was decreased from about 95% to 45% with pH increasing from 6 to 11. Comparing with this study, the percent degradation rate decreased only 6.4% when pH increased from 3.07 to 11.00. This distinction of pH influence was mainly ascribed to the nature of surface construction of iron species and the role of the supporters in which the acidic environment would enhance the catalytic ability of α-FeOOH within the resin [24].

3.3.2. Effect of oxidant and catalyst

The influence of catalyst loading and hydrogen peroxide concentrations on the heterogeneous photo Fenton degradation of E2 by α-FeOOHR were also investigated with different levels of α-FeOOHR catalyst loading (1.0 g/L, 2.5 g/L and 5.0 g/L) and H_2O_2 oxidant concentration (0 mmol/L, 0.97 mmol/L and 9.7 mmol/L). Figs. 5 and 6 show that an increase of E2 conversion with increase of catalyst loading and oxidant concentration. The increase of both variables has led to an enhancement of the photocatalytic performance for

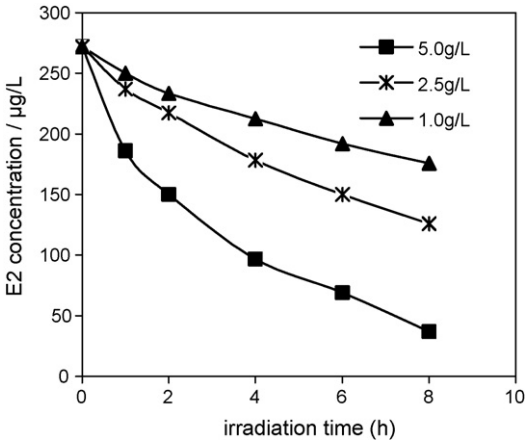

Fig. 5. The effect of catalyst on photodegradation of E2. $[E2]_0 = 272$ μg/L; $[H_2O_2] = 9.7$ mmol/L; pH 7.47; $T = 20°C$; [α-FeOOHR] = 5 g/L, 2.5 g/L, 1.0 g/L.

heterogeneous Fenton reaction. In Fig. 5, the photodegradation efficiency of E2 increased from 35.4% to 86.4% with increased α-FeOOHR loading when H_2O_2 concentration was 9.7 mmol/L after 8 h reaction. In Fig. 6, the photodegradation efficiency of E2 increased from 53.8% to 86.4% with increased H_2O_2 concentration when α-FeOOHR loading was 5.0 g/L. The decomposition rate of E2 is directly related to the levels of catalyst loading and oxidant concentrations. A significant removal of E2 with conversion of 86.4% was obtained using highest catalyst (5.0 g/L) and highest oxidant concentration (9.7 mmol/L).

In Fig. 6, the residual concentration of E2 was 126.8 μg/L after 8 h photodegradation by α-FeOOHR when initial H_2O_2 was not added. It shows that E2 could experience photodegradation though no addition of H_2O_2. This demonstrates that some substitution of H_2O_2 by O_2 can occur [39]. Usually, the presence of oxygen would reduce the quantum yield of ferrous production from ferric ions thus limited the extent of degradation of organics [15]. However, in this study the influence of oxygen somehow showed a positive impact on photodegradation.

Iron species leaching from α-FeOOHR were also investigated during the heterogeneous photo-Fenton degradation of E2 in order to ascertain the strength and stability of α-FeOOH supported in the matrix of resin. Figs. 7 and 8 illustrate the influence of catalyst loading and H_2O_2 concentration on dissolved iron concentrations in the solution during the photodegradation with time. In Fig. 7, dissolved iron species increased from 0 mg/L to 0.95 mg/L after 8 h reaction when photocatalyst α-FeOOHR loading increased from 1.0 g/L to 5.0 g/L for a given H_2O_2 concentration. Also in Fig. 8, dissolved iron species increased from 0.16 mg/L to 0.95 mg/L after 8 h reaction when H_2O_2 concentration increased from 0 mmol/L to 9.7 mmol/L for a given α-FeOOHR loading. The leached iron concentration increased with the increase of H_2O_2 and α-FeOOHR concentrations. This behavior appeared to be the same as that of heterogeneous catalytic Fenton like reaction under dark conditions in which the more significant metal leaching phenomenon was observed for higher concentration of H_2O_2 [40]. In batch reactor, Chou and Huang [41] also discovered that total dissolved iron increased with time during the oxidation of benzoic acid by H_2O_2 with γ-FeOOH at all pH range. However, some contradictory viewpoints were reported. Martínez et al. [32] reported that lower iron leaching showed a general decreasing trend as oxidant concentration was increased. This phenomenon could be attributed to the shielding effect of surrounding metal–H_2O_2 complex species which prevented photoinduced leaching phenomenon by UV–vis irradiations. The reason of iron leaching phenomenon may be related with the nature of catalyst.

In the present study, the stable photocatalytic efficiency, less leached iron species, the strength and stability of α-FeOOHR were further supported by 13 repetitive experiments of E2 photodegradation by α-FeOOHR in presence of H_2O_2. The results showed average concentration of E2 after 8 h reaction was 35.4 μg/L slightly different from that of the first time E2 residual concentration was 36.9 μg/L; while the leached iron

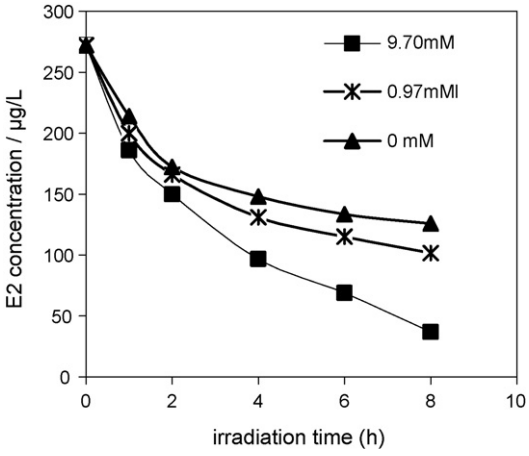

Fig. 6. The effect of oxidant on photodegradation of E2 by α-FeOOHR with time. $[E2]_0 = 272$ μg/L; [α-FeOOHR] = 5 g/L; pH 7.47; $T = 20°C$; $[H_2O_2]$ = 9.7 mmol/L, 0.97 mmol/L and 0 mmol/L.

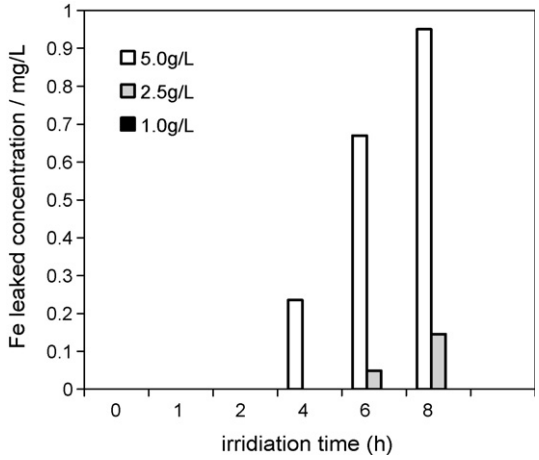

Fig. 7. The effect of catalyst on iron leakage during photodegradation of E2. $[E2]_0 = 272$ μg/L; $[H_2O_2] = 9.7$ mmol/L; pH 7.47; $T = 20°C$; [α-FeOOHR] = 5 g/L, 2.5 g/L, 1.0 g/L.

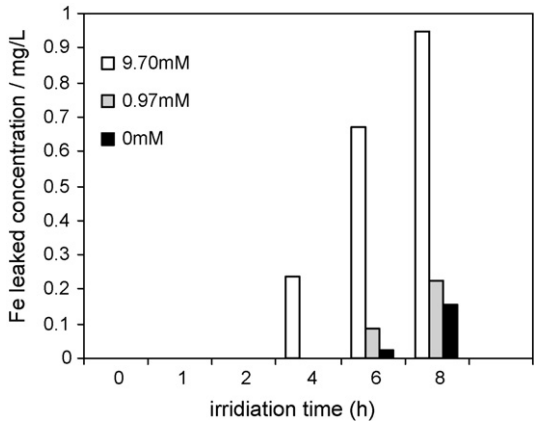

Fig. 8. The effect of oxidant on iron leakage during photodegradation of E2. $[E2]_0 = 272$ μg/L; [α-FeOOHR] = 5 g/L; pH 7.47; $T = 20°C$; $[H_2O_2]$ = 9.7 mmol/L, 0.97 mmol/L and 0 mmol/L.

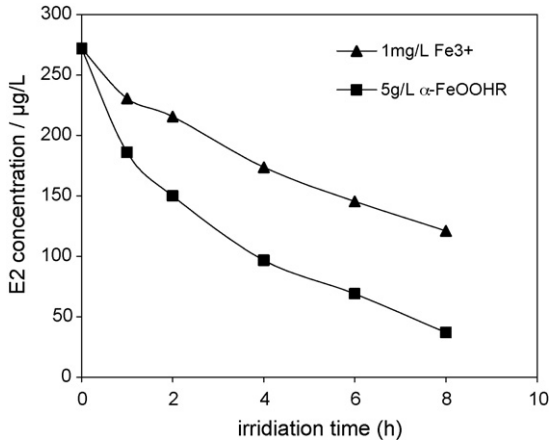

Fig. 9. The effect of homogeneous and heterogeneous catalysis on photodegradation of E2. $[E2]_0 = 272$ μg/L; $[H_2O_2] = 9.7$ mmol/L; pH 7.47; $T = 20°C$; [α-FeOOHR] = 5 g/L; $[Fe^{3+}] = 1.0$ g/L.

average concentration was 0.53 mg/L. So the results demonstrated that the α-FeOOHR has relatively stable photoactivity and mechanic stability and strength for photodegradation of E2 under weak light irradiation and oxidant H_2O_2. It is worth to mention that the α-FeOOHR can be directly used during whole repetitive photo experiments without any regeneration. The proprieties of α-FeOOHR, i.e. high and stable photoactivity, less leached iron, easily separation and no need to be regenerated will make the adsorbent more attractive.

3.4. Influence of homogeneous Fenton

We observed the dissolution of iron into the solution of α-FeOOHR photodegradation experiments with time. Mcbride reported the leached iron was generated via electron transfer [42] while Chou reported increasing leached iron concentrations with pH < 4.0 were due to the reductive dissolution of FeOOH [43]. To understand whether dissolved iron from catalyst would contribute significantly to the decomposition of E2, the dissolved iron concentration was measured after experiments. The photocatalytic decomposition rate of E2 was about 86.4% and the highest total leaking iron concentration measured was 0.95 mg/L (<1.0 mg/L) after 8 h reaction photodegradation reaction in the presence of 5 g/L α-FeOOHR (0.5 g Fe^{3+}/L) and 9.7 mM H_2O_2 at initial pH 7.47. The control homogeneous photo-Fenton experiments (using 1 mg Fe^{3+}/L as catalyst) results showed that the catalytic performance of Fe^{3+} is less than that of heterogeneous photo-Fenton experiment (Fig. 9). The decomposition rate of E2 at this level of dissolved iron concentration was about 46.3% after 8 h reaction. In this study, the leached iron species may quickly hydrolyze and age relative quickly to more stable (less soluble) particulate iron oxyhydroxides forms, which were ascribed to very little photocatalytic activity [15]. The generation of hydroxyl radicals was mainly due to the heterogeneous photocatalysis by α-FeOOHR according to following mechanism [29] (*K* means rate constant). This heterogeneous photo-Fenton reaction was initiated by the formation of peroxide complex species with Fe(III) active sites on the catalyst surface. Then the surface iron complex undergoes a cleavage under UVA irradiation leading to the generation of Fe(II) species and hydroxyl radical. Since the Fe(II) complex is unstable and is followed by Fe(II) reoxidation by H_2O_2 and other radicals:

$$\equiv Fe^{III} - OH + H_2O_2 \xrightarrow{K_1} (H_2O_2)S$$

$$(H_2O_2)s \xrightarrow{K_2} \equiv Fe^{II\bullet}O_2H + H_2O$$

$$\equiv Fe^{II\bullet}O_2H \xrightarrow{K_3} Fe^{II} + {}^{\bullet}O_2H$$

$$\equiv Fe^{II} + H_2O_2 \xrightarrow{K_4} \equiv Fe^{III} - OH + {}^{\bullet}OH + H_2O$$

$$HO_2^{\bullet} \leftrightarrow H^+ + O_2^{\bullet -}$$

$$(H_2O_2)s + \frac{HO_2^{\bullet}}{O_2{}^{\cdot -}} \xrightarrow{K_0} \equiv Fe^{III} - OH + \frac{H_2O}{OH^-} + {}^{\bullet}OH + O_2$$

On the other hand, the heterogeneous photo-Fenton reaction was suggested to be initiated by the formation of a precursor surface complex of H_2O_2 with surface iron centers. The surface iron is immobilized and octahedrally coordinated by O^{2-} and OH^-. The O–O bond of the surface complex undergoes a cleavage under UV irradiation leading to the generation of Fe(IV) species and hydroxyl radical. Since the Fe(IV) complex is unstable, it reacts immediately with H_2O forming another active hydroxyl radical. The photolysis of Fe(III) generates Fe(II), followed by Fe(II) reoxidation by H_2O_2 [19].

Though experiencing different photodegradation pathways, they have a same point, i.e. this heterogeneous photo-Fenton catalyst of all experiences an iron cycling occurred mostly on the catalyst surface. Iron species are therefore recycled directly on the catalyst without significant diffusion into the solution phase [19,23]. The hydroxyl radicals could thus attack the organics adsorbed on the surface of catalyst and lead to the degradation and mineralization without experiencing the homogeneous Fenton pathway induced by dissolving iron species. Because of a rather limited concentration of leached iron in the solution in this study, i.e. the leached iron < 0.25 mg/L after 4 h photodegradation. The activity of the catalyst α-FeOOHR is mainly contributed by the

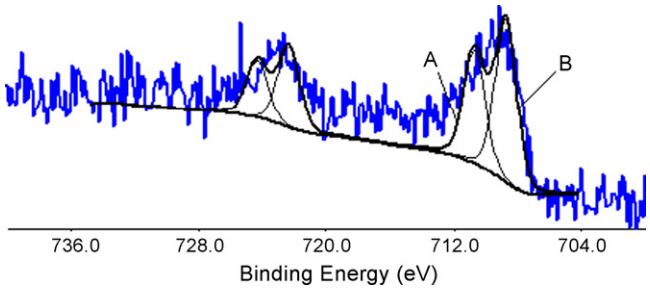

Fig. 10. XPS spectrum of α-FeOOHR after degradation of E2 (Fe 2p line). Component A is due to Fe^{3+} surface species, whereas component B is due to Fe^{2+} species.

heterogeneous catalysis. Chou et al. [43] also reported that the homogeneous catalysis was insignificant at pH > 4.4 when oxidizing Benzoic acid by γ-FeOOH because the outlet total iron concentrations were very low (i.e. <1.5 mg/L), so heterogeneous catalysis played a major role in the reaction. He et al. [19] reported the highest total dissolved iron concentration measured in the presence of 0.5 g/L goethite was up to 1.12 mg/L. The decomposition rate of MY10 at this level of dissolved iron concentration was tested to be two orders of magnitude lower than the rate observed in the presence of iron oxide particles at pH 9. So the homogeneous photo-Fenton reaction in the bulk solution contributes little to the degradation of organic compounds.

The XPS results of the α-FeOOHR samples before and after use during the E2 photodegradation are presented in Fig. 10 and Table 2. Analysis of the results led to a few interesting observations and proved the photodegradation occurred on the surface of catalyst. The most interesting points are probably the presence of two oxidation states of surface iron species, two doublets of Fe 2p with an intensity ratio of 1:2.6, and a splitting energy of about 13.6 eV in samples before photodegradation. The major component is found to be Fe^{3+}, the typical α-FeOOH crystal, which contributes to ∼72% of the total iron surface atoms, while ∼28% of the total iron surface atoms are in the Fe^{2+} state. The 2p line of the α-FeOOHR is very broad and can be deconvoluted into two components with line position at 710.4 eV and 712.2 eV [44]. These two components correspond to the Fe^{2+} and Fe^{3+} species, respectively. For the sample after E2 degradation, the intensity ratio of Fe^{2+}/Fe^{3+} species was found to be 59:41. Whereas, for the sample before E2 degradation, the intensity ratio of Fe^{2+}/Fe^{3+} species was found to be 28:72. Hence, the observation supports the conclusion that α-FeOOH participate in oxidation–reduction reaction during E2 photodegradation. Another observation is that the surface of the α-FeOOH particle on the resin is more strongly hydroxylated, as reflected in the OH surface component observed at 531.4 eV. The intensity of the surface hydroxyl signal is very high. Through these surface hydroxyl groups, E2 can interact with α-FeOOH and undergo photocatalytic decomposition.

Table 2
Binding energy of Fe 2p, O 1s and C 1s elements and atomic surface concentration of detected elements for α-FeOOHR catalysts

	Binding energy (eV)			
	Fe $2p_{1/2}$	Fe $2p_{3/2}$	O 1s	C 1s
Before	710.35	725.77	532.5, 531.4, 530.2	284.6
After	710.44	725.86	532.6, 531.4, 530.1	284.6

	Atomic surface concentration (%)					
	Fe^{2+}	Fe^{3+}	H_2O_{ads}	OH_{surf}	O_{oxides}	C
Before (Fe 2p, 1.36)	27.9%	72.1%	5.1	18.7	3.9	71.0
After (O, 2.00)	59.0%	41.0%	6.5	20.2	4.5	66.8

4. Conclusions

The paper demonstrated that α-FeOOHR could be a highly efficient catalyst to reduce E2 concentration from aquatic environment. E2 in aqueous were decomposed relatively quickly by α-FeOOHR under relatively weak UV illumination (0.3 mW/cm^2) within a wide pH range. The photodegradation process mainly occurred on the surface of the α-FeOOHR, which experienced an iron recycling with insignificant iron leaching. The novel α-FeOOHR catalysts would be of great importance for industrial use due to their high photoactivity, high photocatalytic stability, little iron leaching, easy physical separation, no need to be regeneration and low cost.

Acknowledgements

The present research supported by National University of Singapore and NSF of China (no. 20707006) and PCRRF07002 are greatly appreciated.

References

[1] S. Jobling, M. Nolan, C.R. Tyler, G. Brighty, J.P. Sumpter, Environ. Sci. Technol. 32 (1998) 2498.
[2] F. Ingerslev, E. Vaclavik, B. Halling-Sorensen, Pure Appl. Chem. 75 (2003) 1881.
[3] S. Safe, Environ. Health Perspect. 103 (1995) 346.
[4] G. Ying, R.S. Kookana, Y. Ru, Environ. Int. 28 (2002) 545.
[5] S.F. Arnold, D.M. Klotz, B.M. Collins, P.M. Vonier Jr., L.J. Guillette, J.A. McLachlan, Science 272 (1996) 1489.
[6] C.E. Purdom, P.A. Hardiman, V.J. Bye, N.C. Eno, C.R. Tyler, J.P. Sumpter, Chem. Ecol. (1994) 8275.
[7] C. Desbrow, E.J. Routledge, G.C. Brighty, J.P. Sunoter, M. Waldock, Environ. Sci. Technol. 32 (1998) 1549.
[8] C.J. Andrew, J.P. Sumpter, Environ. Sci. Technol. 35 (2001) 4697.
[9] Y. Zhang, J.L. Zhou, Water Res. 39 (2005) 3991.
[10] H.M. Coleman, B.R. Eggins, J.A. Byrne, F.L. Palmer, E. King, Appl. Catal. B: Environ. 24 (2000) 1.
[11] M.C. Heather, I.A. Mohamed, R.E. Brian, L.P. Fiona, Appl. Catal. B: Environ. 55 (2005) 23.
[12] Y. Ohko, K. Iuchi, C. Niwa, T. Tatsuma, T. Nakashima, T. Iguchi, Y. Kubota, A. Fujishima, Environ. Sci. Technol. 36 (2002) 4175.
[13] C. Ooka, H. Yoshida, M. Horio, K. Suzuki, T. Hattori, Appl. Catal. B: Environ. 41 (2003) 313.
[14] K. Wu, Y. Xie, J. Zhao, H. Hisao, J. Mol. Catal. A: Chem. 144 (1999) 77.
[15] P. Simon, Advanced Oxidation Processes for Water and Wastewater Treatment, IWA Publishing, 2004.
[16] P. Mazellier, M. Bolte, J. Photochem. Photobiol. A: Chem. 132 (2000) 129.

[17] J. Bandara, J.A. Mielczarski, A. Lopez, J. Kiwi, Appl. Catal. B: Environ. 34 (2001) 321.
[18] P.T. Marc, G.M. Verónica, A.B. Miguel, G. Jaime, E. Santiago, Appl. Catal. B: Environ. 47 (2004) 219.
[19] J. He, W. Ma, J. Zhao, J.C. Yu, Appl. Catal. B: Environ. 39 (2002) 211–220.
[20] K. Fajerwerg, H. Debellefontaine, Appl. Catal. B: Environ. 10 (1996) L229.
[21] S. Parra, L. Guasaquillo, O. Enea, E. Mielczarski, J. Mielczarski, P. Albers, L. Kiwi-Minsker, J. Kiwi, J. Phys. Chem. B 107 (2003) 7026.
[22] J. Fernandez, M.R. Dhananjeyan, J. Kiwi, Y. Semuna, J. Hilborn, J. Phys. Chem. B 104 (2000) 5298.
[23] R.L.J. Vaughan, B.E. Reedb, Water Res. 39 (2005) 1005.
[24] D. Wang, Z. Liu, F. Liu, X. Ai, X. Zhang, Y. Cao, J. Yu, T. Wu, Y. Bai, T. Li, X. Tang, Appl. Catal. A: Gen. 174 (1998) 25.
[25] M.J. DeMarco, A.K. SenGupta, J.E. Greenleaf, Water Res. 37 (2003) 164.
[26] X. Guo, F. Chen, Environ. Sci. Technol. 39 (2005) 6808.
[27] X. Lv, Y. Xu, K. Lv, G. Zhang, J. Photochem. Photobiol. A: Chem. 173 (2005) 121.
[28] M. Cheng, W. Ma, J. Li, Y. Huang, J. Zhao, Y. Wen, Y. Xu, Environ. Sci. Technol. 38 (2004) 1569.
[29] S. Lin, M.D. Gurol, Environ. Sci. Technol. 32 (1998) 1417.
[30] T. Beata, W.M. Antoni, I. Michio, T. Masahiro, Appl. Catal. B: Environ. 63 (2006) 215.
[31] R. Parag, Gogate, B.P. Aniruddha, Adv. Environ. Res. 8 (2004) 501.
[32] F. Martínez, G. Calleja, J.A. Melero, R. Molina, Appl. Catal. B: Environ. 60 (2005) 181.
[33] D. Zhou, F. Wu, N. Deng, X. Wu, Water Res. 38 (2004) 4107.
[34] B. Neppolian, J.S. Park, H. Choi, Ultrason. Sonochem. 11 (2004) 273.
[35] I.A. Katsoyiannis, A.I. Zouboulis, Water Res. 36 (2002) 5141.
[36] U. Hoins, L. Charlet, H. Sticher, Water Air Soil Pollut. 68 (1993) 241.
[37] A. Albert, E.P. Serjeant, The determination of ionization constants: a laboratory manual, Chapman and Hall, London, 1971.
[38] S. Chou, C. Huang, Appl. Catal. A: Gen. 185 (1999) 237.
[39] B. Utset, J. Garcia, J. Casado, X. Domènech, J. Peral, Chemosphere 47 (2000) 1187.
[40] J.L. Sotelo, G. Ovejero, F. Martínez, J.A. Melero, A. Milieni, Appl. Catal. B: Environ. 47 (2004) 281.
[41] S. Chou, C. Huang, Chemosphere 38 (1999) 2719.
[42] McBride, Soil Sci. Soc. Am. J. 51 (1987) 1466.
[43] S. Chou, C. Huang, Y. Huang, Environ. Sci. Technol. 35 (2001) 1247.
[44] M. Dhananjeyan, E. Mielczarski, K. Thampi, P. Buffat, M. Bensimon, A. Kulik, J. Mielczarski, J. Kiwi, J. Phys. Chem. 105 (2001) 12046.